

Astrophysics of gravitational wave sources

Lecture 8: Final phases of stellar evolution

Ondřej Pejcha

ÚTF MFF UK

Why do stars shine?

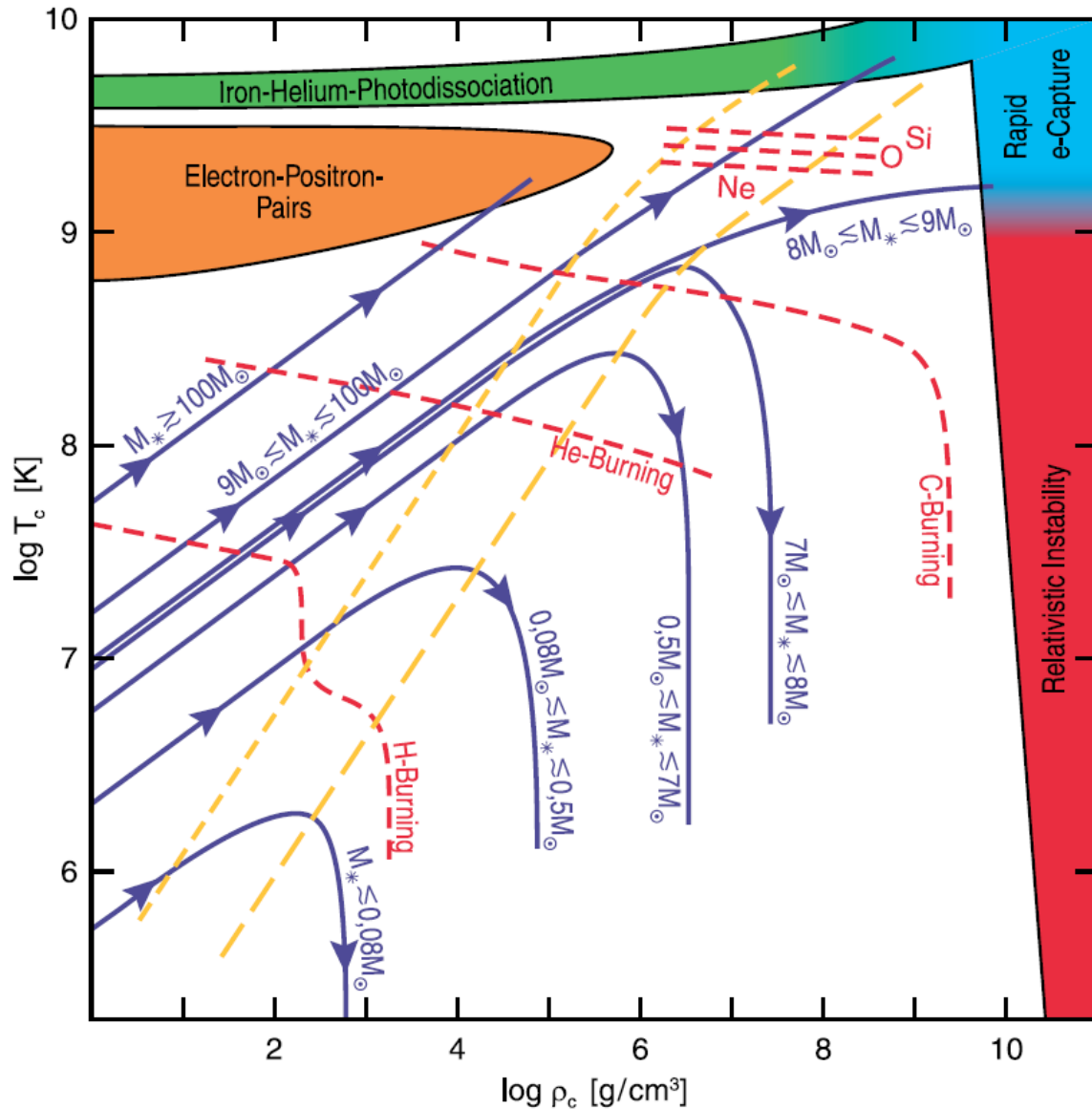
(correct answers only)

Separation of stellar timescales

- Dynamical (free-fall, sound-crossing) timescale
- (Viscous timescale)
- Thermal (Kelvin-Helmholtz) timescale
- Nuclear timescale

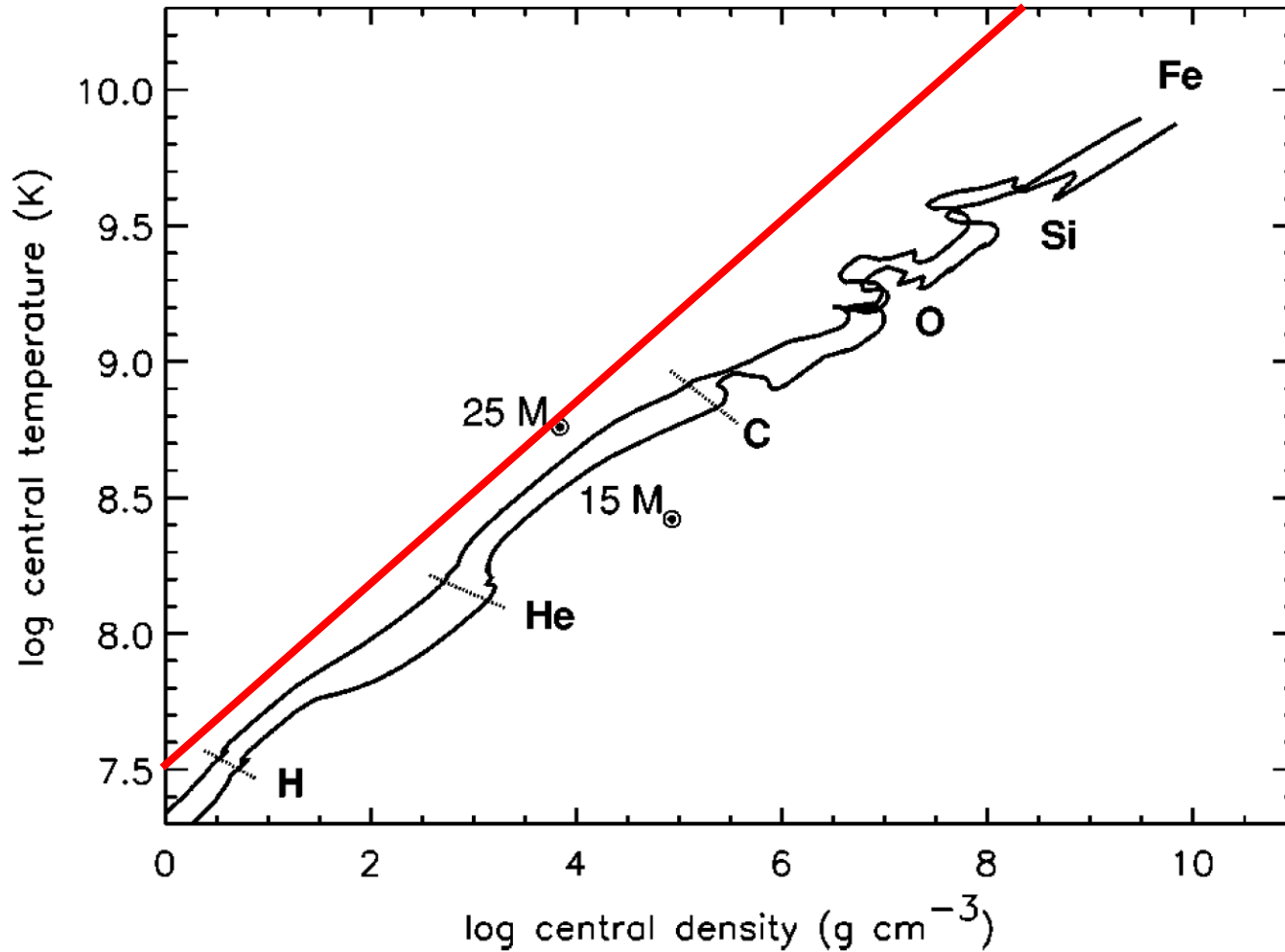
Single star evolution before core-collapse

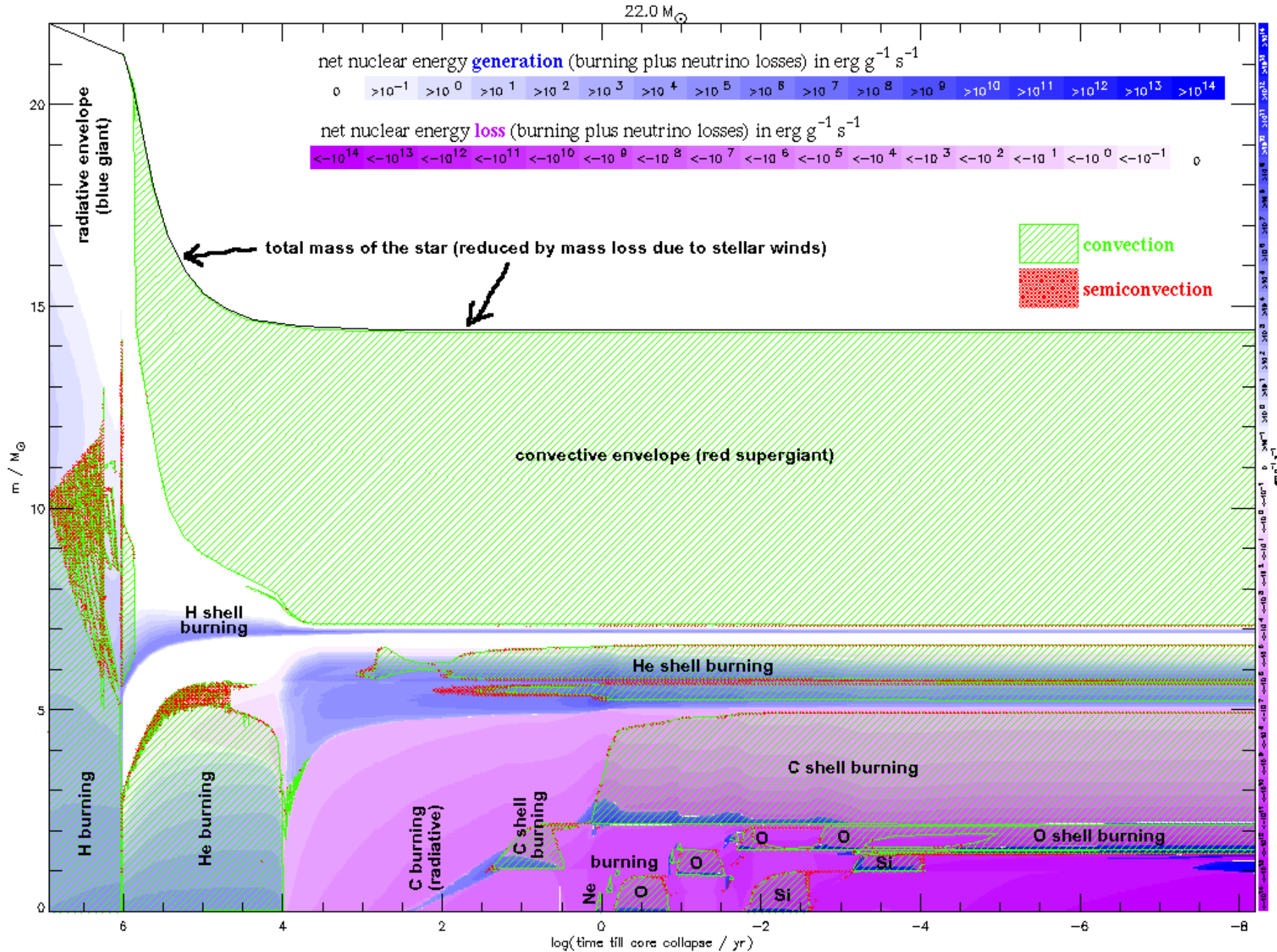
Central temperature and pressure



Single star evolution before core-collapse

Central temperature and pressure

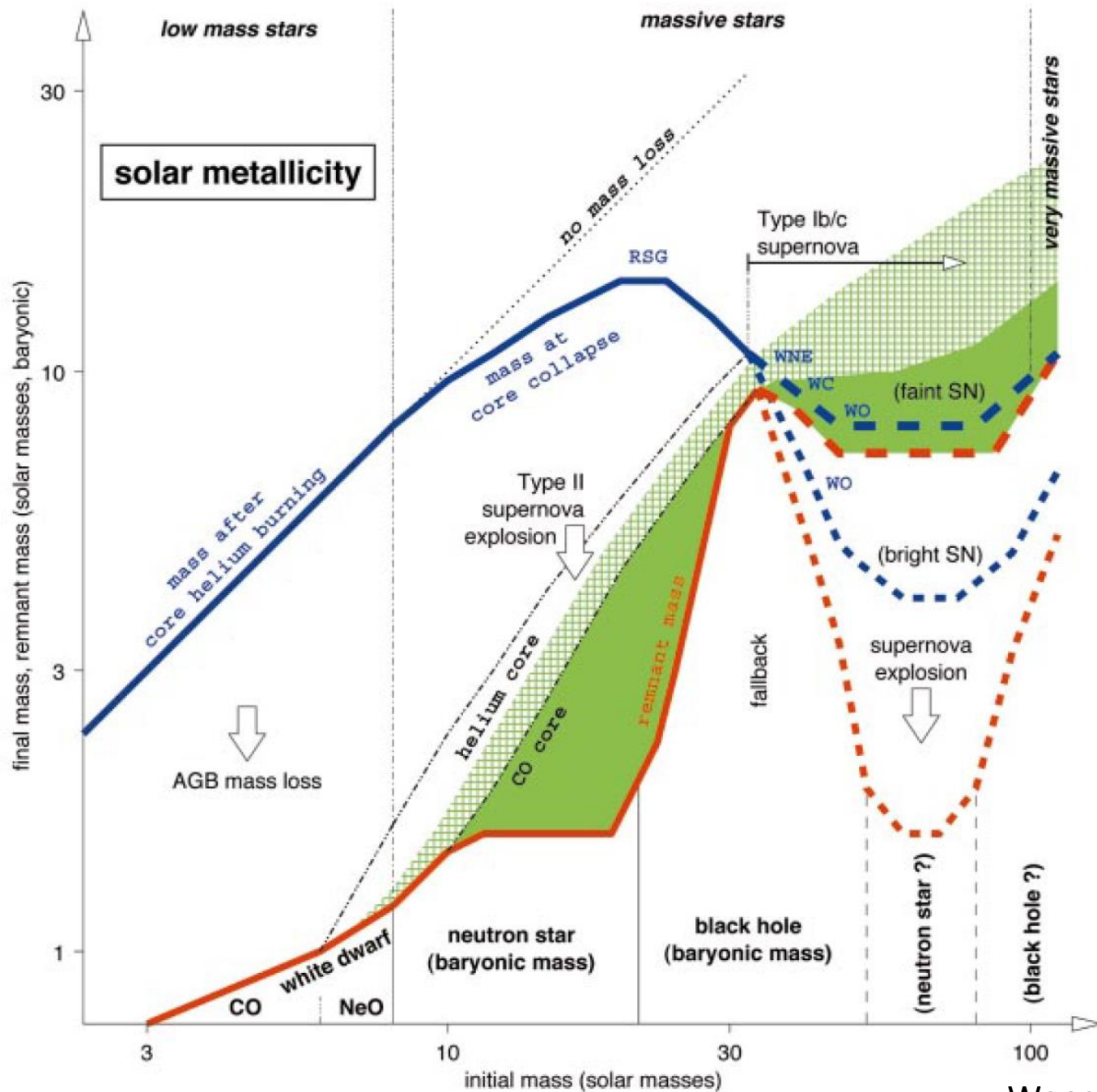




A. Heger website 2sn.org

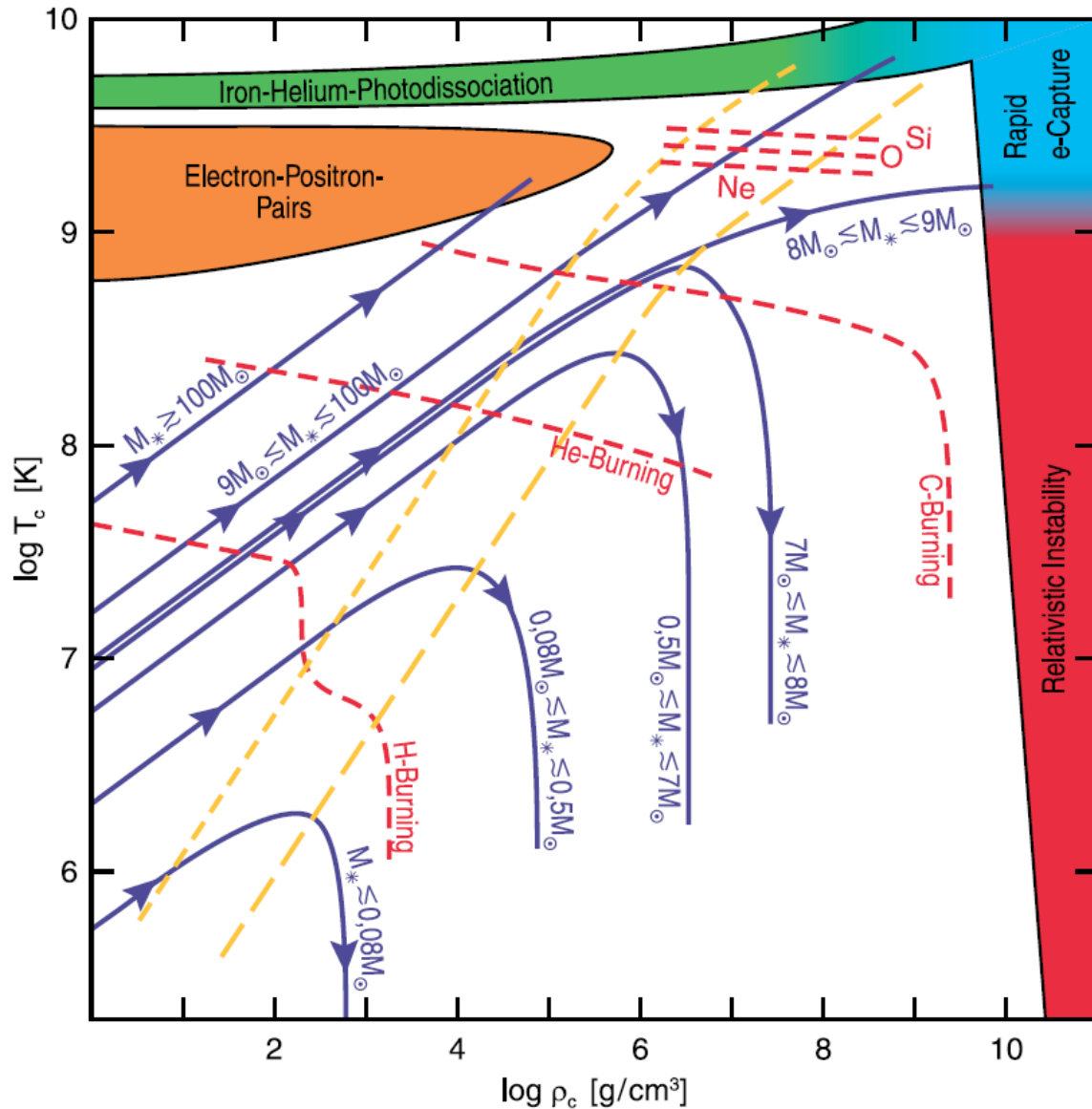
Physical processes inside massive star

- Convection
 - Mixing length theory, but convective and nuclear timescales comparable
 - Mixing as a diffusive process
- Semi-convection
 - Schwarzschild – instability only due to temperature/pressure gradients
 - Ledoux – also takes into account chemical composition
 - Unstable by Schwarzschild & stable by Ledoux = semi-convection
 - Diffusion coefficient uncertain
- Overshoot mixing
 - Modeled by diffusion
- Rotation & magnetic fields
 - Coupling of core to envelope – affected by mass loss
- Mass loss
- Neutrino losses
 - Mostly due to thermal processes (T^9), later due to neutronization (T^6)
 - Accelerates evolution (\sim day timescale for silicon)



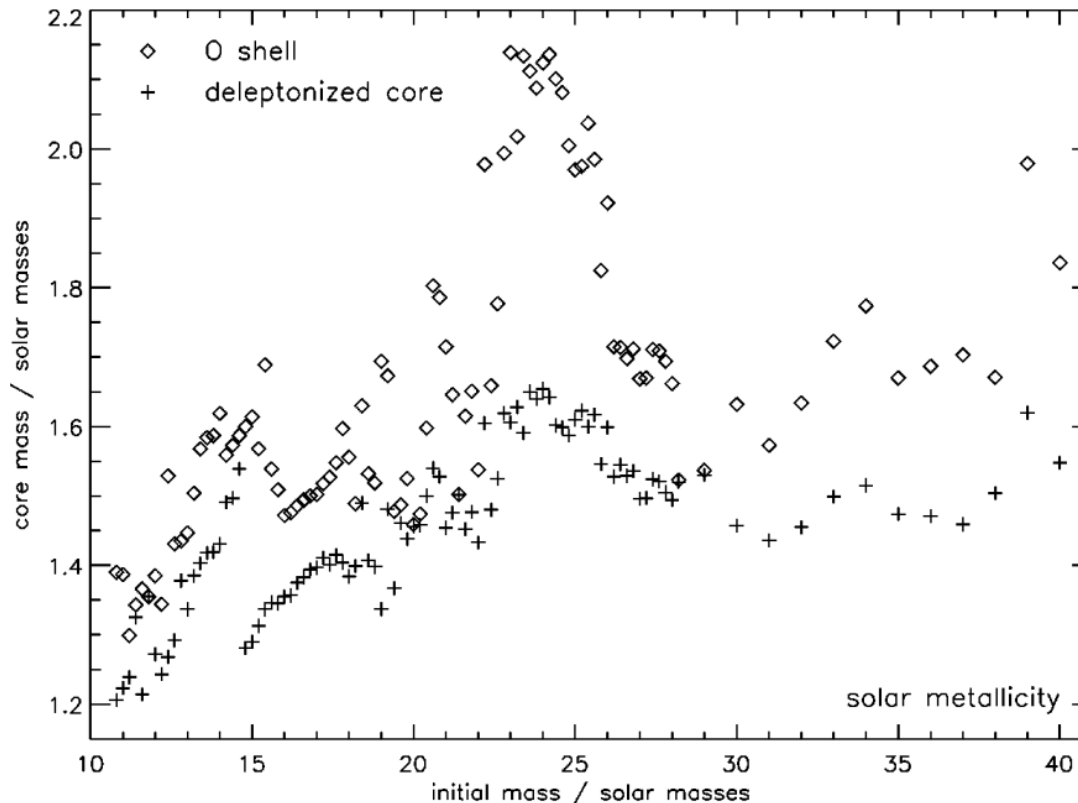
Single star evolution before core-collapse

Central temperature and pressure



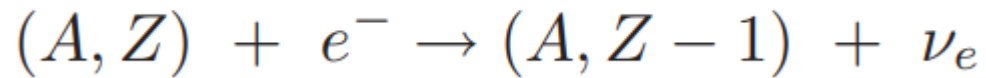
Chandrasekhar mass

- Chemical composition
- Thermal structure of the core (nonzero entropy)
- Coulomb corrections (electrons have charge)
- Nonzero pressure at outer boundary of the core
- Special and general relativistic corrections
- Effective Chandrasekhar mass between 1.2 and 1.8 M_{sun} (approximately)



Acceleration of collapse

- Electron capture when electron Fermi energy higher than energy levels of nuclei (few MeV) -> removes electrons



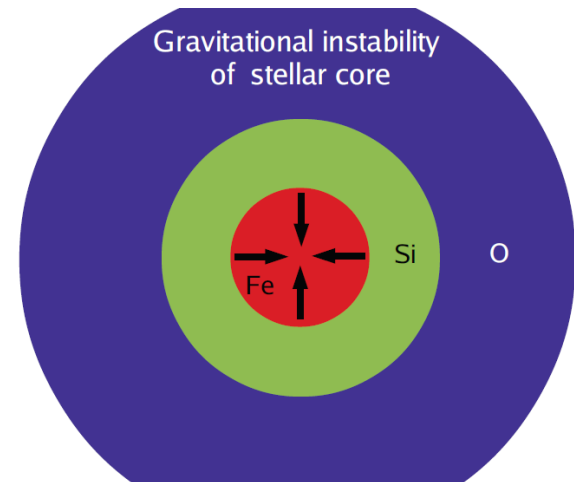
$$\epsilon_F \geq M(A, Z - 1) - M(A, Z)$$

- Photodisintegration to alpha particles
(requires binding energy)

1 erg = 10^{-7} J

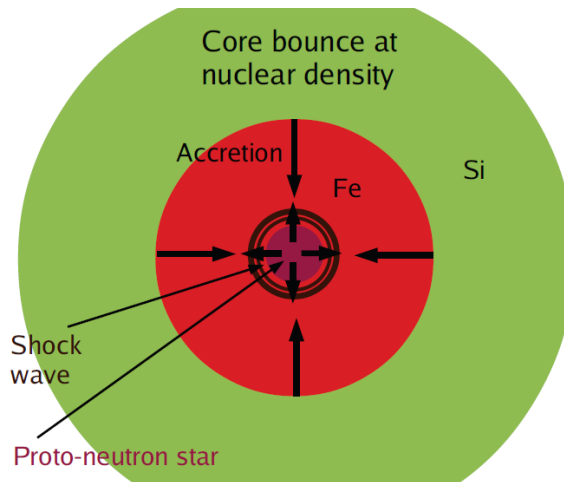
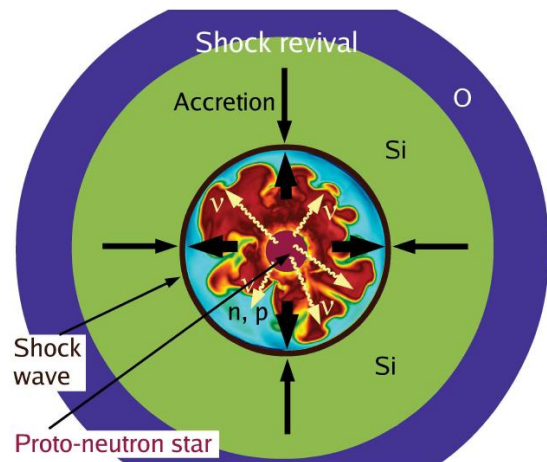
Massive star death

$1 L_{\odot} = 3.9 \times 10^{33}$ ergs/s



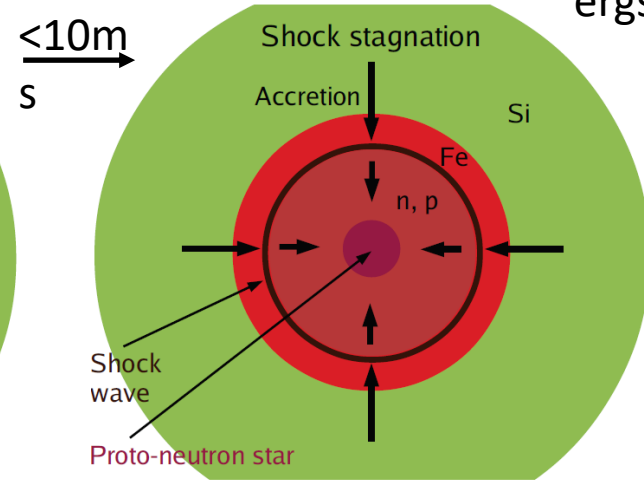
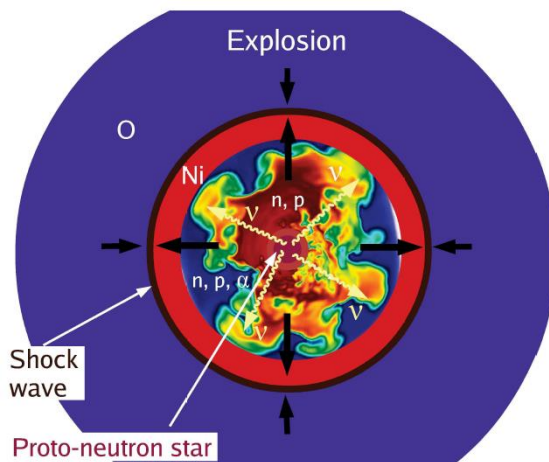
$M_{\text{initial}} > 8 M_{\odot}$
Collapse from WD size $\sim 0.3s$

Reason not fully understood



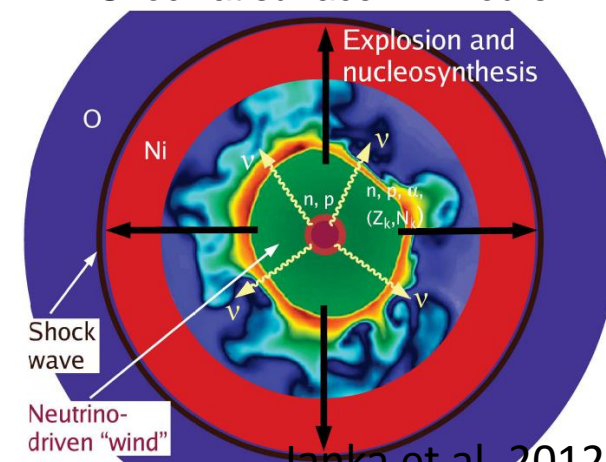
Proto-neutron star ~ 60 km
Binding energy $\sim 3 \times 10^{53}$ ergs

All NS binding energy released
before 10-100s



Stalled shock at 100-200 km
Neutrino cooling $\sim 10^{52}$ ergs/s
Duration up to ~ 1 s

Explosion energy $\sim 10^{51}$ ergs
 $10^{-3} - 10^{-1} M_{\odot}$ of Nickel-56
Shock at surface in \sim hours



Janka et al. 2012

O'Connor & Ott (2011)

Ugliano et al. (2012)

Ertl et al. (2016)

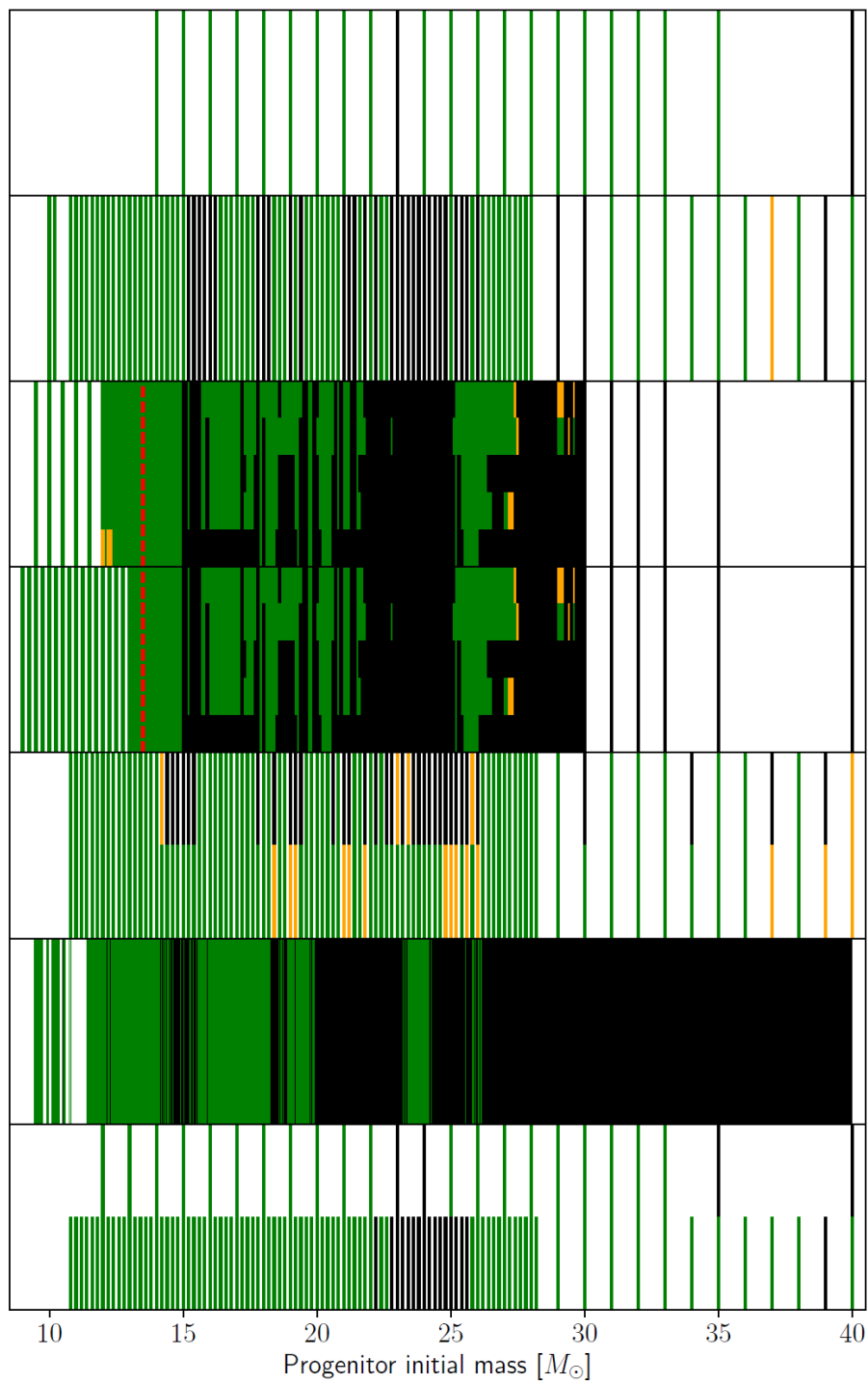
Sukhbold et al. (2016)

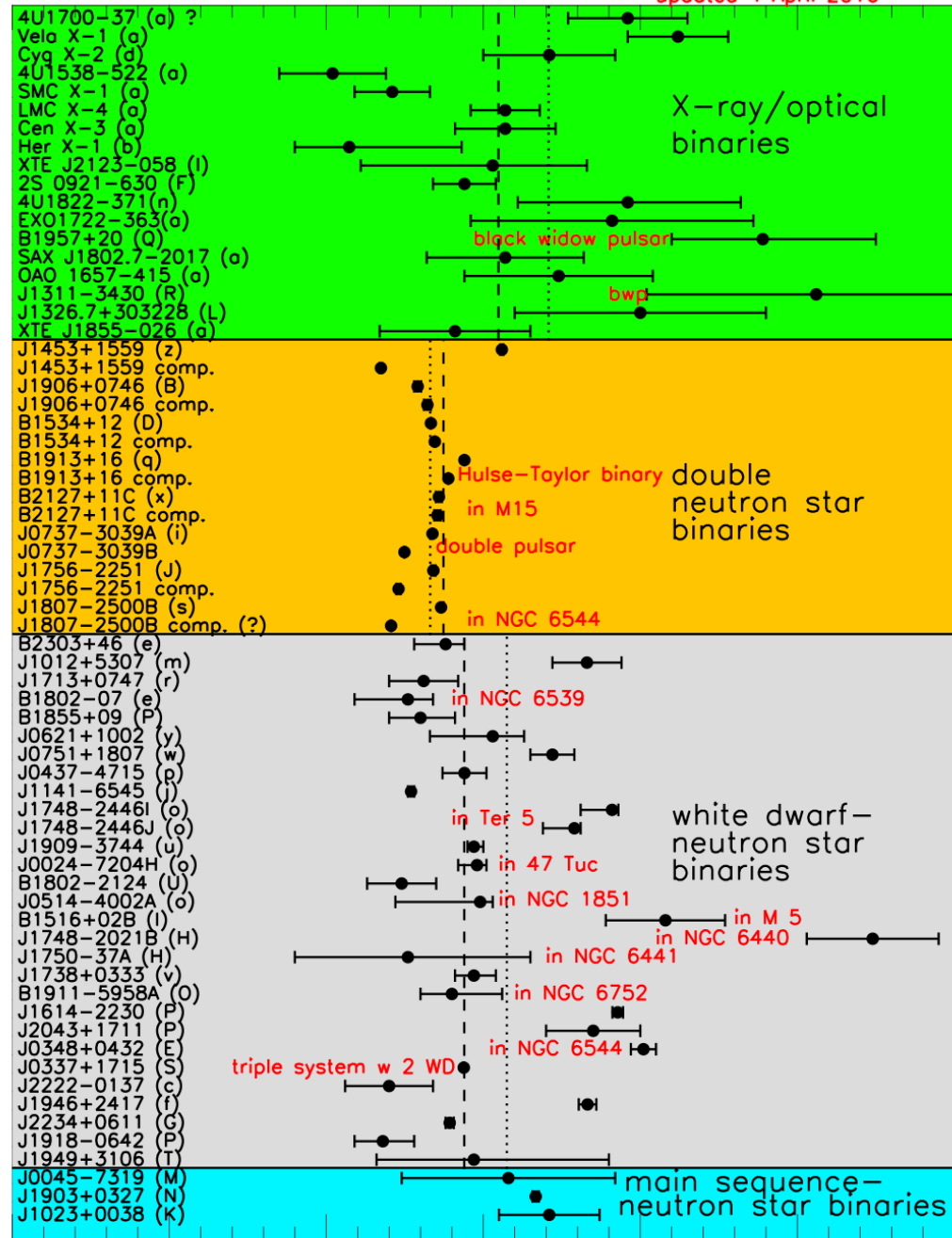
Pejcha & Thompson (2015)

Müller et al. (2016)

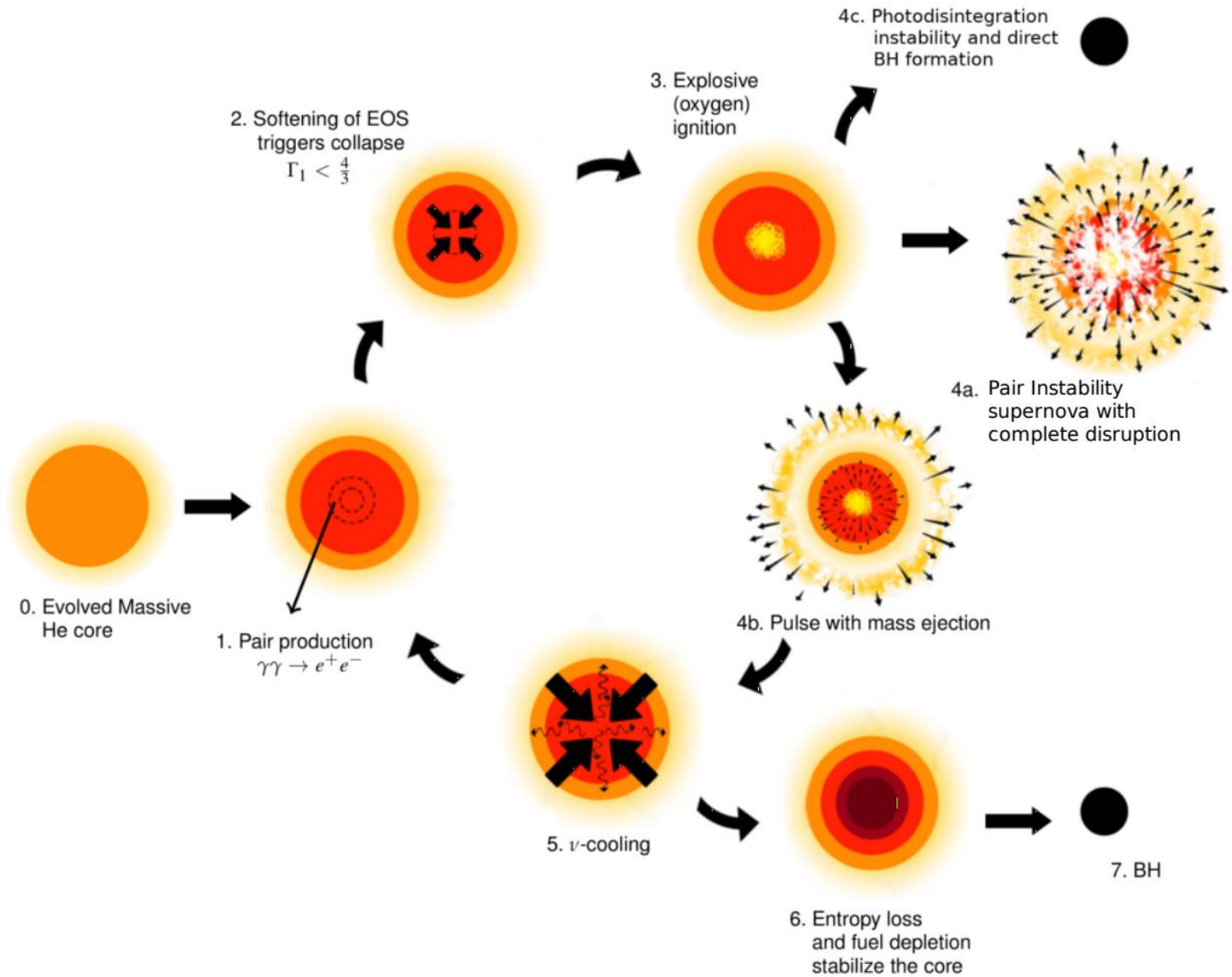
Ebinger et al. (2019)

N20
S19.8
W15
W18
W20
N20
S19.8
W15
W18
W20
(a)
(b)
WH07
WHW02





0.0 0.5 1.0 1.5 2.0 2.5 3.0
Neutron star mass (M_{\odot})



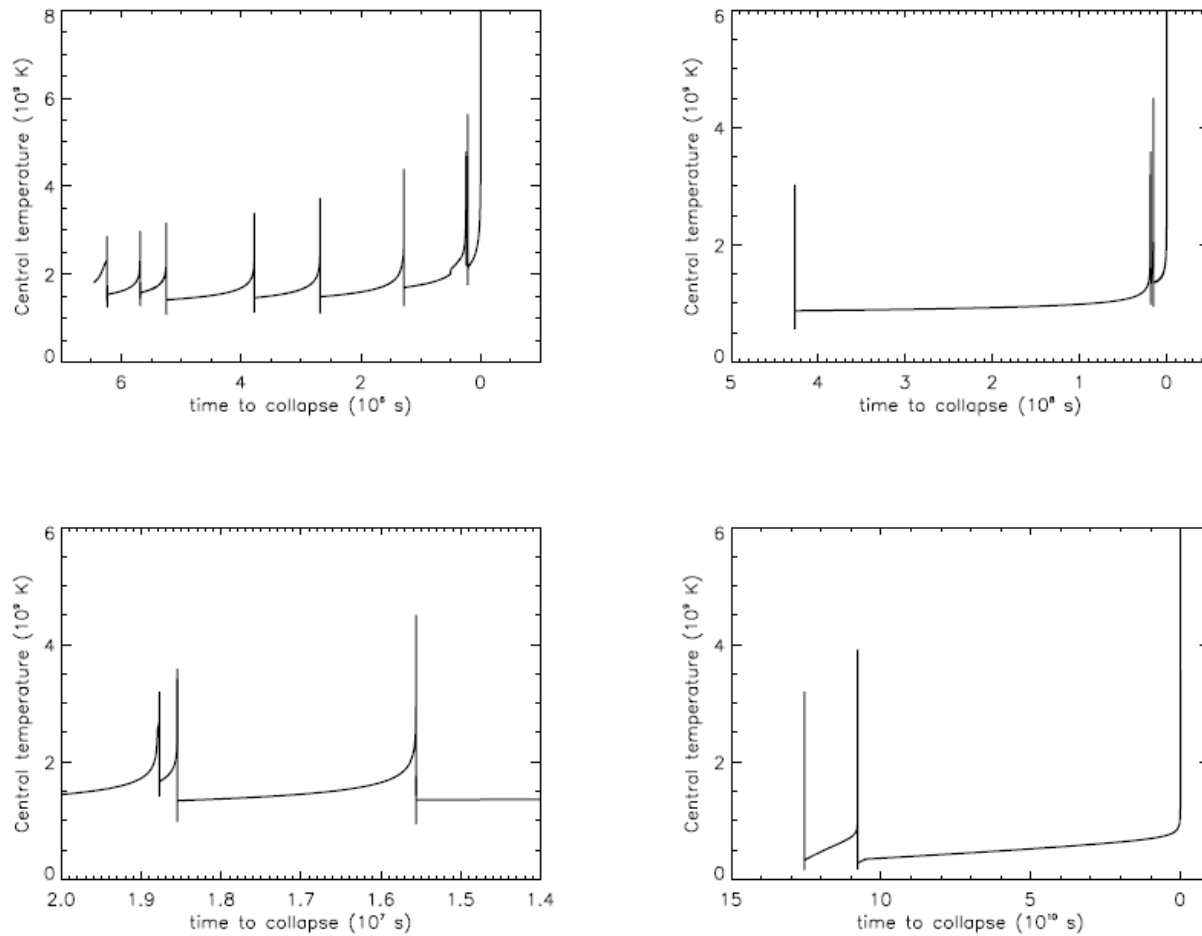


Fig. 2 Pair-driven pulsations cause rapid variations in the central temperature (10^9 K) near the time of death for helium cores of 32, 36, 40, 44, 48, 52 (on two different time scales) and 56 M_{\odot} (left to right; top to bottom). The log base 10 of the time scales (s) in each panel are respectively 4, 4, 5, 5, 6, 8, 7, and 10. The last rise to high temperature marks the collapse of the iron core to a compact object. More massive cores have fewer, less frequent, but more energetic pulses. All plots begin at central carbon depletion.

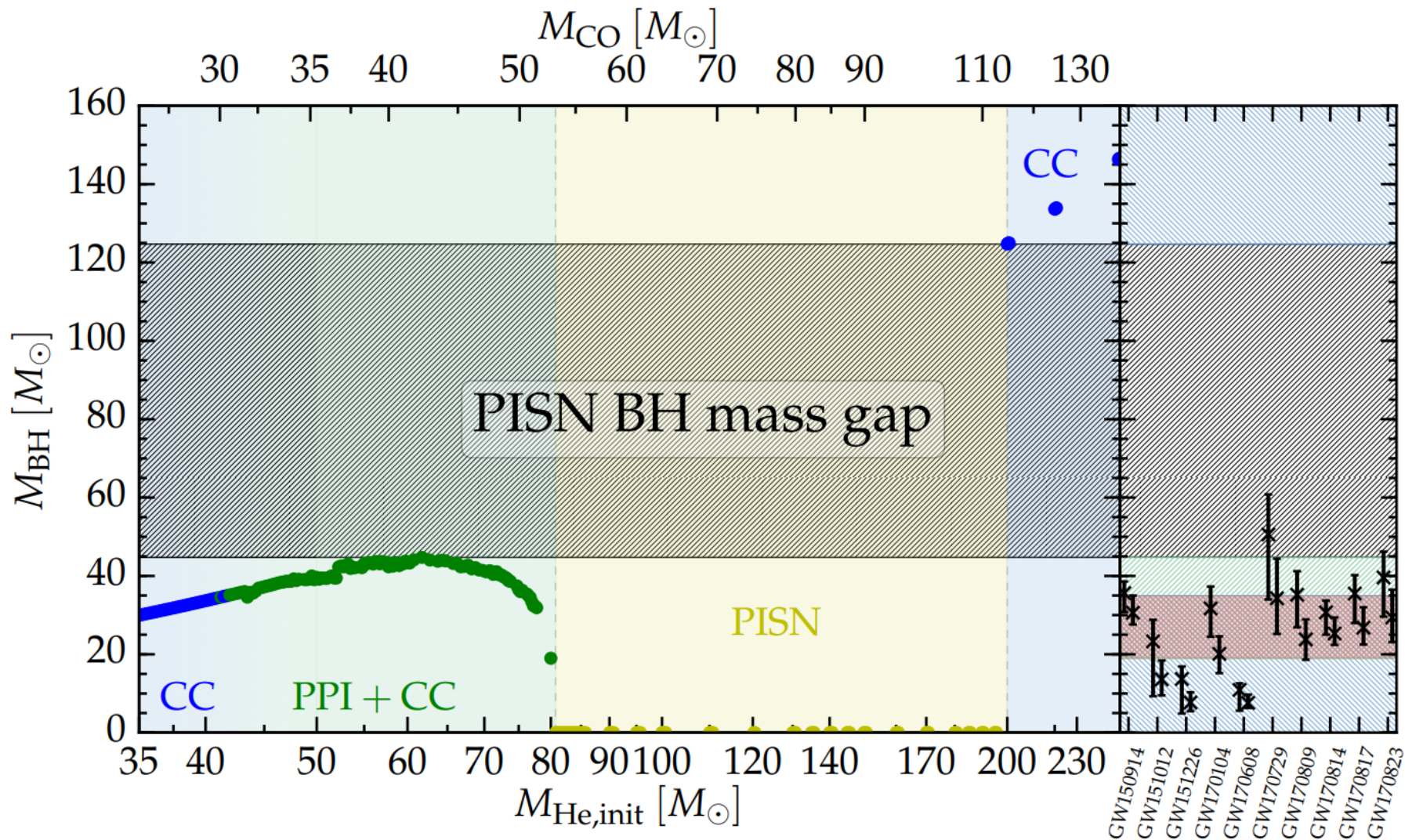


Fig. 2. Final BH masses as a function of the initial He core mass. The scale in the horizontal direction is logarithmic. The colors in the background indicate the approximate range for each evolutionary path, see also Section 3. The right panel shows the masses inferred from the first ten binary BH mergers detected by LIGO/Virgo, with a red shade to emphasize the overlap between PPI and CC, and green and blue hatches to indicate the fate of the progenitor in different BH mass ranges.

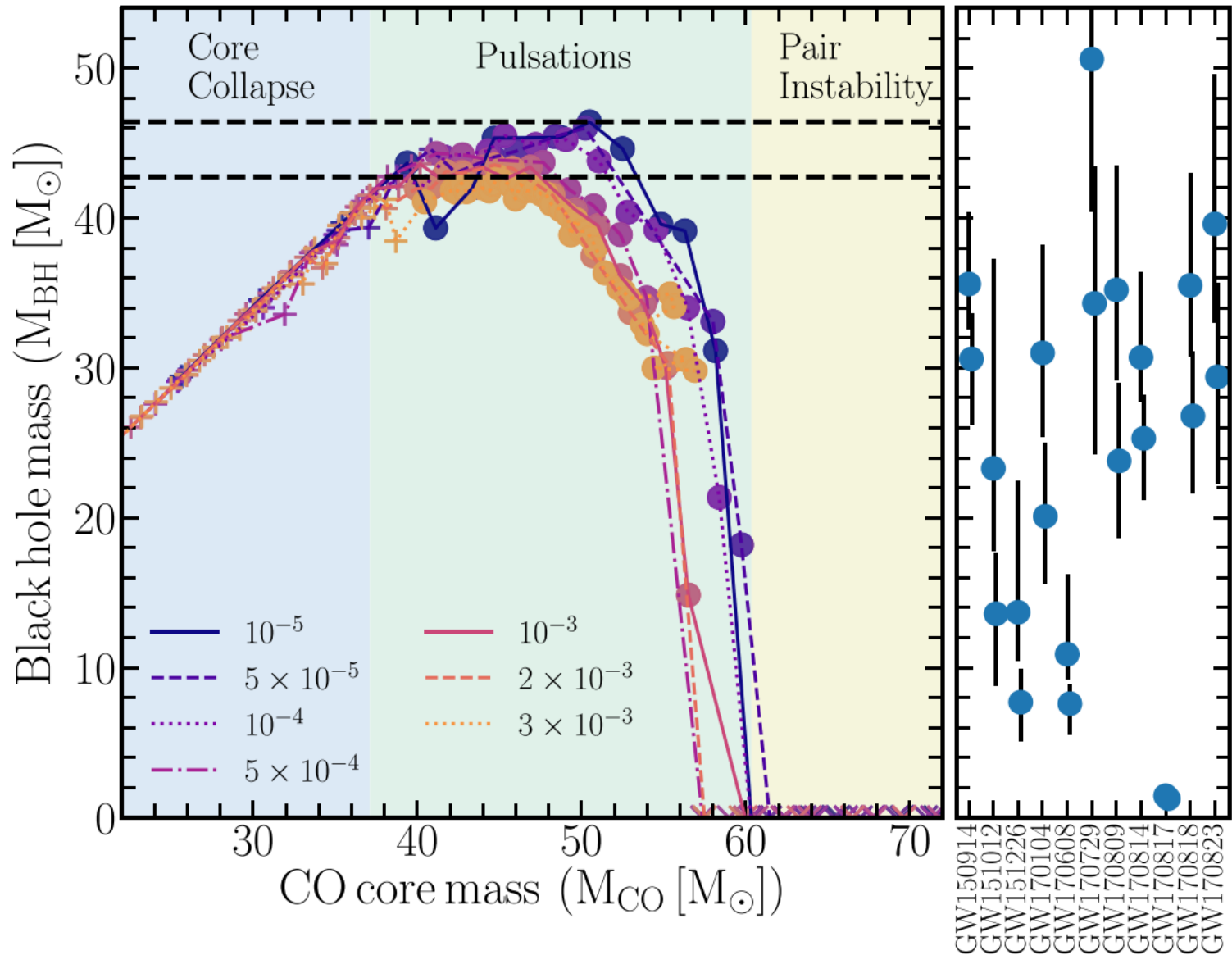







Figure 2. Mass of final BH as a function of the CO core mass for different metallicities. Circles denote models that underwent at least one pulse, pluses evolved directly to CC, and crosses undergo a PISN. The left (blue) region denotes where models undergo CC, the middle (green) region denotes PISNe, while the right (yellow) region denotes PISNe, as determined by stars with $Z = 10^{-5}$. Points in the right panel show the current median mass estimates for the double compact objects detected by LIGO/VIRGO with their 90% confidence intervals (Abbott et al. 2019a). Dashed horizontal lines emphasize the maximum spread in the locations for the edge of the BH mass gap, or in other words the spread in the maximum BH mass below the PISN BH mass gap.



CrossMark

OPEN ACCESS

On Stellar Evolution in a Neutrino Hertzsprung–Russell Diagram

Ebraheem Farag¹ , F. X. Timmes^{1,2} , Morgan Taylor¹ , Kelly M. Patton³ , and R. Farmer⁴ ¹ School of Earth and Space Exploration, Arizona State University, Tempe, AZ 85287, USA; ekfarag@asu.edu² Joint Institute for Nuclear Astrophysics—Center for the Evolution of the Elements, USA³ Department of Physics and Astronomy, Colby College, Waterville, ME 04961, USA⁴ Anton Pannenkoek Institute for Astronomy and GRAPPA, University of Amsterdam, NL-1090 GE Amsterdam, The Netherlands*Received 2019 November 26; revised 2020 March 4; accepted 2020 March 10; published 2020 April 23*

Abstract

We explore the evolution of a select grid of solar metallicity stellar models from their pre-main-sequence phase to near their final fates in a neutrino Hertzsprung–Russell diagram, where the neutrino luminosity replaces the traditional photon luminosity. Using a calibrated MESA solar model for the solar neutrino luminosity ($L_{\nu,\odot} = 0.02398 \cdot L_{\gamma,\odot} = 9.1795 \times 10^{31} \text{ erg s}^{-1}$) as a normalization, we identify $\simeq 0.3 \text{ MeV}$ electron neutrino emission from helium burning during the helium flash (peak $L_{\nu}/L_{\nu,\odot} \simeq 10^4$, flux $\Phi_{\nu,\text{He flash}} \simeq 170 (10 \text{ pc}/d)^2 \text{ cm}^{-2} \text{ s}^{-1}$ for a star located at a distance of d parsec, timescale $\simeq 3$ days) and the thermal pulse (peak $L_{\nu}/L_{\nu,\odot} \simeq 10^9$, flux $\Phi_{\nu,\text{TP}} \simeq 1.7 \times 10^7 (10 \text{ pc}/d)^2 \text{ cm}^{-2} \text{ s}^{-1}$, timescale $\simeq 0.1$ yr) phases of evolution in low-mass stars as potential probes for stellar neutrino astronomy. We also delineate the contribution of neutrinos from nuclear reactions and thermal processes to the total neutrino loss along the stellar tracks in a neutrino Hertzsprung–Russell diagram. We find, broadly but with exceptions, that neutrinos from nuclear reactions dominate whenever hydrogen and helium burn, and that neutrinos from thermal processes dominate otherwise.